Deriving daily evapotranspiration from remotely sensed instantaneous evaporative fraction over olive orchard in semi-arid Morocco

Joost Hoedjes, Ghani Chehbouni, Frédéric Jacob, J. Ezzahar, Gilles Boulet

Deriving daily evapotranspiration from remotely sensed instantaneous evaporative fraction over olive orchard in semi-arid Morocco

J.C.B. Hoedjes [a], A. Chehbouni [a,*], F. Jacob [b], J. Ezzahar [c], G. Boulet [a]

[a] IRD/CESBIO, UMR: CNES-CNRS-UPS-IRD, 18 Avenue Edouard Belin, 31401 Toulouse Cedex 9, France
[b] IRD, UMR LISAH, 2 Place Viala, 34060 Montpellier, France
[c] University Cadi-Ayyad, Marrakech, Morocco

Summary   Hydrology and crop water management require daily values of evapotranspiration ET at different time-space scale. Sun synchronous optical remote sensing, which allows for the assessment of ET with high to moderate spatial resolution, provides instantaneous estimates during satellites overpass. Then, usual solutions consist of extrapolating instantaneous to daily values by assuming that evaporative fraction EF is constant throughout the day, providing that daily available energy AE is known. The current study aims at deriving daily ET values from ASTER derived instantaneous estimates, over an olive orchard in a semi-arid region of Moroccan. It has been shown that EF is almost constant under dry conditions, but it depicts a pronounced concave up shape under wet conditions. A new heuristic parameterization is then proposed, which is based on the combination of routine daily meteorological data for characterizing atmospheric dependence, and on optical remote sensing based estimates of instantaneous EF values to take into account the dependence on soil and vegetation conditions. Using the same type of approach, a similar parameterization is next developed for AE. The validation of both approaches shows good performances. The overall method is finally applied to ASTER data. Though performances are reasonably good, their moderate reduction is ascribed to errors on remotely sensed variables. Future works will focus on method portability since its empirical formulation does not account for the direct stomatal response to water availability, as well as on application over different surface and climate conditions.
© 2008 Published by Elsevier B.V.

* Corresponding author. Tel.: +33 (0)5 61 55 8197; fax: +33 (0)5 61 55 85 00.
  E-mail addresses: joost.hoedjes@cesbio.cnes.fr (J.C.B. Hoedjes), ghani@cesbio.cnes.fr (A. Chehbouni), frederic.jacob@ supagro.inra.fr (F. Jacob), j.ezzahar@ucam.ac.ma (J. Ezzahar), gilles.boulet@cesbio.cnes.fr (G. Boulet).

Introduction

Estimates of regional evapotranspiration (ET) are of crucial need for climate studies, weather forecasts, hydrological surveys, ecological monitoring, and water resource management (Van den Hurk et al., 1997; Su, 2000; Bastiaanssen et al., 2000). Given that distributed hydrological models can accurately estimate basin scale runoff while poorly reproducing other hydrological cycle components, intermediate processes such as soil moisture and thus ET have to be well simulated (Chaponnière et al., 2007). Within semiarid agricultural regions, which hydrological cycle is strongly influenced by ET through crop water consumption, a precise ET estimation is of importance for water saving through efficient irrigation practices (Allen, 2000; Ohmura and Wild, 2002; Porporato et al., 2004; Wild et al., 2004). Among the several research programs designed to develop efficient irrigation management tools in arid and semi-arid zones, the SUDMED (Chehbouni et al., in press-a) and IRRIMED (http://www.irrimed.org) projects have taken place in southern Mediterranean regions, to assess the spatio-temporal variability of water needs and consumption for irrigated crops under water limited conditions.

Optical satellite remote sensing is a promising technique for estimating instantaneous and daily ET at global and regional scale, via surface energy budget closure. The methods proposed in the literature range from simple and empirical approaches, to complex and data consuming ones (Glenn et al., 2007). Among the complex methods are Soil Vegetation Atmosphere Transfer (SVAT) models, which describe the diurnal course of heat and mass transfers, provided micrometeorological conditions and water/energy balance parameters are documented (Braud et al., 1995; Mahfouf et al., 1995; Olioso et al., 1996; Calvet et al., 1998; Olioso et al., 2005; Coudert et al., 2006; Gentine et al., 2007). Among the simple approaches are the simplified relationship, which links daily ET to midday near surface temperature gradient (Jackson et al., 1977). In the same vein, the FAO-56 method expresses daily ET using crop coefficients derived from vegetation indexes, but needs to be calibrated with ground measurements (Duchemin et al., 2006; Er-Raki et al., 2007a, Yang et al., 2006). Between complex and empirical approaches, compromising solutions are energy balance models. They compute at satellite overpass instantaneous ET as the residual term of energy budget, once net radiation, soil heat flux and sensible heat flux are derived (Bastiaanssen et al., 1998; Norman et al., 2003; Su, 2002; Caparrini et al., 2003, 2004; French et al., 2005; Crow and Kustas, 2005; Allen et al., 2007; Cleugh et al., 2007; Mu et al., 2007).

Instantaneous values of ET at satellite overpass can be used as diagnostics for surface status (Chandrapala and Wimalasuriya, 2003), or as controls for hydrological models through assimilation schemes (Schuurmans et al., 2003). However, their interest in terms of water management is limited, since the latter requires daily values (Bastiaanssen et al., 2000). Daily ET can be derived from FAO-56 or simplified relationship, but difficulties raise when extrapolating outside the environmental conditions considered for calibration. The ET diurnal course can be inferred assimilating sun synchronous observations into SVAT models, but this is limited by uncertainties when estimating SVAT parameters and initial variables. The ET diurnal course can also be retrieved using geostationary observations, but the kilometric resolutions severely limit water management at the field scale. Probably, the most practical solution is estimating instantaneous values from energy balance models combined with sun synchronous observations, and next extrapolating at the daily scale by presuming generic trends for the diurnal courses of ET and related variables.

Assuming generic trend for the ET diurnal course can consist of approximating the latter by a sine function, given it is similar to that of solar irradiance. However, this method is limited by its empirical character in terms of accuracy (Zhang and Lemeur, 1995). Another possibility is assuming a typical shape for Evaporative Fraction (EF) given Available Energy (AE) is known. The EF is defined as the ratio of ET to AE, and AE is the difference between net radiation and soil heat flux. EF is in deed an important indicator of the surface hydrological history, including wetting and drying events (Shuttleworth et al., 1989; Nichols and Cuenca, 1993). Thus, it was suggested to assume a constant daytime EF, to be used with daily AE for deriving daily ET (Sugita and Brutsaert, 1991; Roerink et al., 2000; Gomez et al., 2005).

Assuming a daytime constant EF is not straightforward, regarding what has been reported from both theoretical and experimental based investigations (Crago, 1996; Crago and Brutsaert, 1996). Zhang and Lemeur (1995) observed EF changes with environmental variables, especially AE and surface resistance. Suleiman and Crago (2004) reported that EF increases with vegetation amount, soil moisture and air dryness. Baldocchi et al. (2004) and Li et al. (2006) reported that stomatal conductance drives EF according to soil moisture since soil dryness tends to decrease both variables. During fair weather conditions over fully vegetated surfaces, Lhomme and Elguero (1999) reported from model simulation a typical concave-up shape for EF, quite constant during midday, and mainly driven by changes in soil moisture and solar energy. Thus, assuming a daytime constant EF equal to the noon value induces underestimations since this value is the lowest of the day. Finally, Gentine et al. (2007) showed that EF diurnal course mainly depends on both evaporative state and vegetation cover. Besides the EF diurnal course, addressing the daytime AE is a delicate issue. Empirical approaches have been proposed to derive it from instantaneous values, mainly approximating AE by a sine function (Jackson et al., 1983; Bastiaanssen et al., 2000). Again, the most adequate solution is using geostationary satellite observations, but the corresponding spatial resolutions make the use of such data complicated for water management at field scale.

In the same context of the investigations discussed above, the present study aims at inferring daily ET from sun synchronous optical remote sensing, with the objective of improving irrigation water management at the field scale. The challenge is then considering an irrigated old olive orchard in central Morocco, characterized by a semi-arid climate, tall trees, and strong soil moisture heterogeneity due to irrigation practices. This challenge was addressed in four steps. We first examine the EF diurnal behavior using Eddy Correlation (EC) measurements, and then quantify errors on daily ET when assuming EF self-preservation.

Second, we parameterize the EF diurnal course using a combination of routinely available meteorological data and a unique ''one shot'' instantaneous EF estimates. Third, we parameterize the AE diurnal cycle from ground based measurements of energy balance, also by considering routine micrometeorological measurements and a single instantaneous estimates of AE. Finally, the proposed parameterizations after being calibrated using ground based data are applied to ASTER data. These different steps are implemented using data collected during the 2003–2004 period. Given that ASTER data was only available in 2003, design and calibration were performed using ground-based 2004 dataset, while validation was performed using the 2003 one.

Site description and experimental setup

The study took place in a semi-arid basin in central Morocco (the Tensift basin, Fig. 1) within the framework of the SUD-MED Program (http://www.irrimed.org/sudmed). In this section, site description and experimental setup are briefly summarized; the reader is referred to Chehbouni et al. (in press-a) for a complete description of both project and site. The regional climate was characterized by low and irregular rainfalls with a 240 mm annual average, an evaporative demand of about 1600 mm per year, and a dry atmosphere with a 56% average humidity. The experiment was carried out between Day Of Year (DOY) 288 in 2002 and DOY 271 in 2004, at the 275 ha Agdal olive orchard, southeastern of Marrakech (31°36′N, 07°58′W). The average height of the olive trees is 6.5 m, the average crown diameter is 6.5 m. The density of the olive trees at our site is about 225 ha^{-1}. Understorey vegetation consists mainly of short weeds, with ground cover ranging from almost no (10–20%) cover to almost complete (70–80%) cover (Hoedjes et al., 2007). The olive trees are irrigated through level basin flood irrigation. For this purpose, each tree is surrounded by a small earthen levy, and water is directed to each tree through a network of ditches (Williams et al., 2004). On average, the irrigation takes approximately 12 days.

The experimental setup collected standard meteorological measurements: wind speed and direction (Young Wp200 anemometer); air temperature and humidity (Vaisala HMP45AC temperature and humidity probe). The instruments were set 9 m above ground (3 m above canopy).
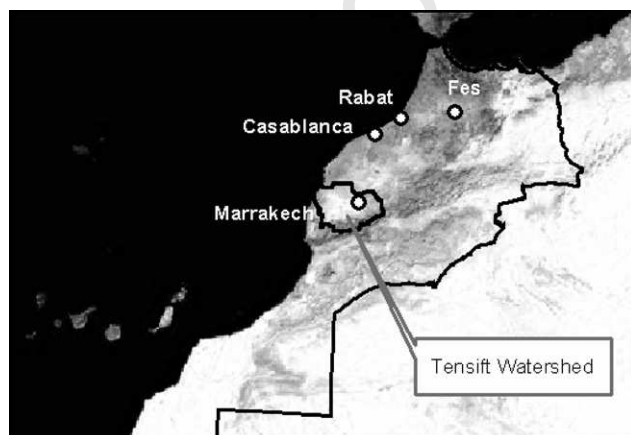

Figure 1   Location of the study area.

The four net radiation components were measured using a Kipp and Zonen CNR1 radiometer, set at an 8.5 m height to embrace vegetation and soil radiances by ensuring the field of view was representative of their respective cover fractions. Soil and vegetation brightness temperatures were measured using two Apogee IRTS-P. The soil heat flux density was measured using heat flux plates (HFT3-L, Campbell Scientific Ltd.) at three locations with contrasting amounts of radiation reaching the soil. The measurement depth was 1 cm. The plates were placed: one below the tree, near the trunk in order not to be exposed to direct solar radiation; one was exposed directly to solar radiation, the last one in an intermediate position. An average of these three measurements was made to obtain a representative value. Soil moisture and temperature were recorded at different depths within the 0–50 cm horizon, using CS616 water content reflectometer and TP107 temperature probes (both Campbell Scientific Ltd.), respectively. Measurements were sampled at 1 Hz, and 30 min averages were stored on CR10X dataloggers (Campbell Scientific Ltd.).

The EC system was installed at a 9.2 m height. During the first three months it included a CSAT 3 3D sonic anemometer (Campbell scientific Ltd.) and a LICOR-7500 open-path infrared gas analyzer (Campbell Scientific Ltd.). Raw data were sampled at a 20 Hz rate, recorded using a CR23X datalogger (Campbell scientific Ltd.). After three months, the LICOR-7500 was replaced by a KH20 Krypton hygrometer (Campbell Scientific Ltd.), and the CR23X was replaced with a CR5000 datalogger (Campbell Scientific Ltd.). The half-hourly fluxes were later calculated off-line using Eddy Covariance processing software 'ECpack', after performing all required corrections for planar fit correction, humidity and oxygen (KH20), frequency response for slow apparatus, and path length integration (Van Dijk et al., 2004).

The analysis showed that the sum of latent and sensible heat flux measured independently by the EC systems was often lower than available energy (AE). The absolute value of average closure was about 8% and 9% of available energy during the 2003 and 2004 seasons, respectively (Er-Raki et al., 2007b). This problem could not be explained neither by mismatching spatial extents for fluxes and AE measurements, nor by uncertainties associated with measurements of soil heat flux and net radiation (Twine et al., 2000; Hoedjes et al., 2002; Chehbouni et al., in press-b, 2007c). Correction was then performed using the approach suggested by Twine et al. (2000), which assumes the energy balance is due to underestimates from EC measurements while the corresponding Bowen ratio is correctly estimated. Based on this assumption, we re-computed sensible and latent heat fluxes by forcing the energy balance closure using the measured AE and Bowen ratio.

ASTER official products (Abrams and Hook, 2002) were downloaded from the Earth Observing System Data Gateway (EDG). Once instrumental effects are removed (Fujisada, 1998; Fujisada et al., 1998; Abrams, 2000), atmospheric corrections are performed using radiative transfer codes documented for atmospheric status (Thome et al., 1998), providing surface reflectance's over the solar domain (bands 1–9) and surface brightness temperatures over the thermal domain (bands 10–14). The latter are next used to derive surface emissivity and radiometric temperature by applying the Temperature Emissivity Separation algorithm (Gillespie
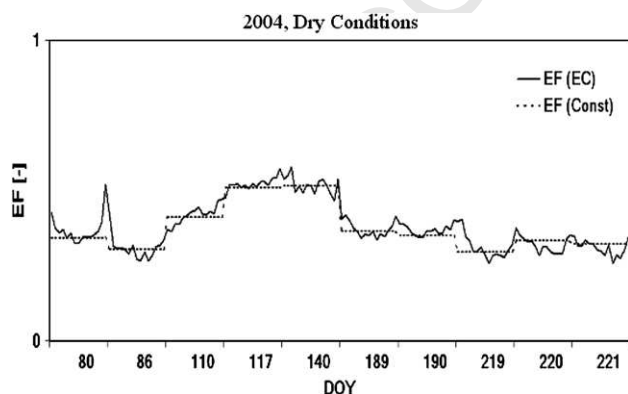
et al., 1998; Schmugge et al., 1998). Six ASTER images were collected over the study area, one in 2002 (DOY 311), and 5 in 2003 (DOY 58, 138, 202, 282 and 289). Spatial resolution is 15 m (respectively 30 m) for visible and near infrared (respectively shortwave) reflectance's, and 90 m for emissivity and radiometric temperature. Higher resolution products were linearly degraded to 90 m, given aggregation effects from spatial heterogeneities could be considered as minor over flat semiarid regions (Jacob et al., 2004; Liu et al., 2006).

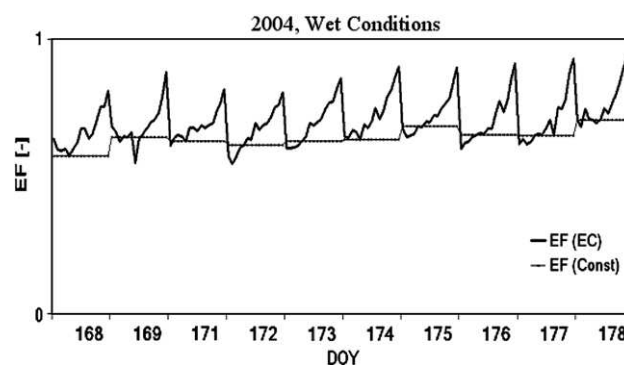## Method design, implementation and assessment

The parameterization is designed and assessed using ground based EC data collected during the 2003–2004 experimental period. ASTER data were only available in 2003. Therefore, design and calibration were performed using the 2004 dataset, whilst validation was performed using the 2003 ground and ASTER dataset. Furthermore, only daytime observations from 09:30 to 16:30 UTC are considered, since the most important latent heat fluxes occur during this period.

EF diurnal course and impact-assessment on ET estimates

In this section we assess the validity of EF self-preservation using the EC data during dry and wet conditions. It is important to mention that dry or wet conditions should normally be characterized by soil moisture conditions. However, since we are dealing with the EF which is influenced by both surface and atmospheric conditions, we preferred instead to use the Bowen Ratio (BR = H/LE) with a threshold value higher (lower) than 1.5 as indicator of dry (wet) conditions. Fig. 2a displays the observed diurnal variations of EF as well as the EF constant value set up to that observed at 11:30 UTC (ASTER time overpass) for 10 cloud free days under dry conditions, selected between DOY 80 and DOY 221 in 2004. The same curves are presented in Fig. 2b, for a 10-day cloud free period in 2004 under wet conditions. It can be seen that that assuming EF self-preservation is valid under dry conditions, since EF is relatively constant despite
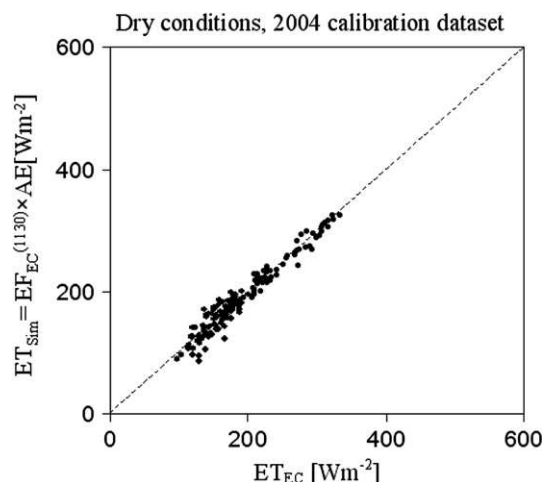

Figure 2b The same as Fig. 2a for 10 wet days following an irrigation event in 2004 (DOY 168–178).

observed some daily variation. But this assumption is not valid under wet conditions, since EF depicts a concave-up shape with a straight decrease in early morning and a sharp increase in late afternoon. Thus, assuming EF is constant and equal to EF @ 11:30 UTC underestimates actual daytime EF and consequently latent heat flux. These results corroborate those reported by Lhomme and Elguero (1999), Suleiman and Crago (2004) and Gentine et al. (2007).

Next, we quantify the errors on daytime ET when assuming a constant EF. The ET diurnal course is estimated combining a daily constant EF and in situ data of AE:

$$ET_{EF,const} = EF^{1130}AE = EF^{1130}(R_n - G) \qquad (1)$$

Fig. 3a and b displays comparisons of half hourly ET values simulated from Eq. (1) against observations for dry and wet conditions in 2004, respectively. As it might be can be expected, assuming EF self-preservation appears to be valid under dry conditions, with an RMSE between observed and simulated ET of 14 W m^{-2} (calibration residual error) and a Nash–Sutcliffe coefficient of 0.94. Under wet conditions, however, assuming a constant EF significantly underestimates ET, with an RMSE between observations and simulations of 46 W m^{-2}, and a Nash-Sutcliffe coefficient of

Figure 2a Eddy Covariance (EC) derived evaporative fraction EF (EC) and constant EF (at 11:30) for 10 selected dry and cloud free days within the 2004 selected between DOY 80 and DOY 221.

Figure 3a Comparison between eddy covariance latent heat flux (ET$_{EC}$) and latent heat flux calculated using EF$_{EC}$ at 11:30 as constant during daytime (ET$_{Sim}$) during the 10 dry days in 2004.

Figure 3b   Comparison between eddy covariance latent heat flux (ET_{EC}) and latent heat flux calculated using EF_{EC} at 11:30 as constant during daytime (ET_{Sim}) during a 10-day period following an irrigation event in 2004.

0.34. Thus, the validity of assuming EF self-preservation depends on soil moisture. It is therefore necessary under wet condition to account for the diurnal cycle of EF to derive accurate estimates of daytime ET.

Parameterizing the EF diurnal cycle

An alternative to assuming EF self preservation is proposed here, through a heuristic approach that parameterizes the EF diurnal cycle. The constraints are accounting for the EF daytime relative stability under dry conditions, and adequately reproducing the EF diurnal course during wet conditions. For operational applications at the irrigation district scale, the dependence must rely on routinely measured parameters which remain reasonably constant at such scale, or on parameters available from remote sensing. Given the EF diurnal cycle depends on both atmospheric forcing and surface conditions (Gentine et al., 2007), parameterizing the diurnal behavior of EF is twofold. First, the diurnal cycles of atmospheric forcing are considered, since atmospheric demand is controlled by incoming radiation, relative humidity and, to a lesser extent, wind speed. Second, we account for land surface heterogeneities potentially available from remotely sensed thermal data, since control on surface temperature is exerted by vegetation characteristics and most importantly by soil moisture status.

Since an increase in EF mainly results from an increase in incoming solar radiation and a decrease in atmospheric humidity (Lhomme and Elguero, 1999; Suleiman and Crago, 2004; Gentine et al., 2007), the first step consists of parameterizing the diurnal shape of EF as a function of the main atmospheric forcing parameters, i.e. incoming solar radiation $S^\downarrow$ and relative humidity RH. The proposed parameterization reads:

$$EF_{Sim} = 1.2 - \left(0.4\frac{S^\downarrow}{1000} + 0.5\frac{RH}{100}\right) \qquad (2)$$

Though Eq. (2) provides a good representation of the relative EF diurnal course, the magnitude and the day-to-day variation of the EF absolute minimum depend on soil moisture conditions. Therefore, the second step aims at incorporating, a daily scaling factor in order to produce the actual day to day variation of EF (EF_{Sim}^{ACT}). In order to use efficiently remote sensing data, this scaling factor r_{EF}^{1130} is expressed as the ratio of simulated to actual EF when ASTER overpasses @ 11:30 UTC:

$$EF_{Sim}^{ACT} = EF_{Sim} r_{EF}^{1130} \qquad (3)$$

with

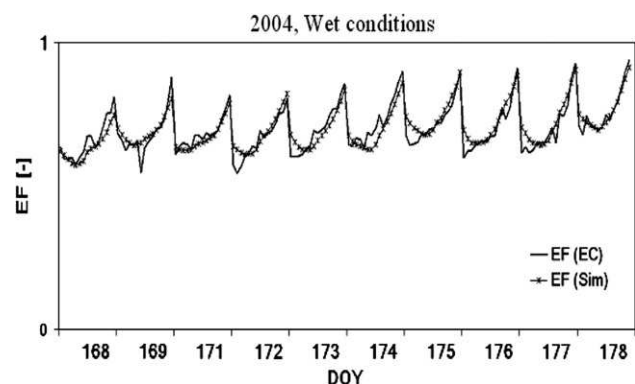$$r_{EF}^{1130} = \frac{EF_{Obs}^{1130}}{EF_{Sim}^{1130}} \qquad (4)$$

For development purposes, EF_{Obs}^{1130} is obtained from EC latent heat observations as well as locally measured AE @ 11:30 UTC, and is written as EF_{Ec}^{1130}. Later on, EF_{Obs}^{1130} will be derived from remote sensing data only, using ASTER data to derive latent heat, and routinely available data to estimate AE; it will be named EF_{ASTER}^{1130}.

To account for the validity of EF self preservation under dry conditions which usually corresponds to Bower ratio values higher than 1.5, the complete EF parameterization becomes:

$$EF_{Sim}^{ACT} = \begin{cases} EF_{Sim} r_{EF}^{1130} & \beta^{1130} \leqslant 1.5 \\ & \text{for} \\ EF_{Obs}^{1130} & \beta^{1130} \leqslant 1.5 \end{cases} \qquad (5)$$

To assess the performance of this proposed parametrisation, we present in Fig. 4 chronicles of measured (EFEC) and simulated (EF_{Sim}) EF, for the same 10-day period than Fig. 2b (2004, wet conditions). Compared to the constant daytime EF as provided in Fig. 2b, EF_{Sim} approximates in a better way the observed EF diurnal variation (EFEC). In order to evaluate the resulting improvement in terms of evaporation estimates, latent heat flux is derived from parameterized EF and in situ observations of AE during the day:
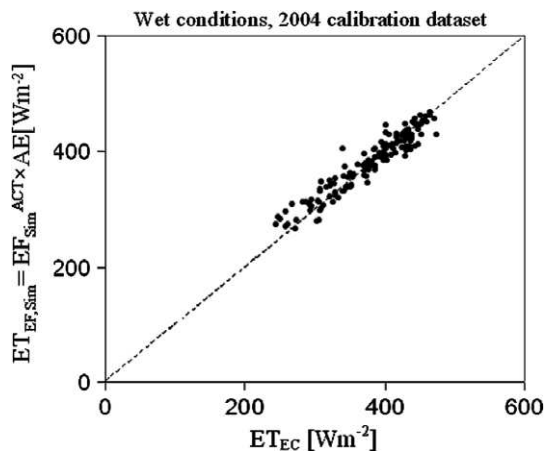
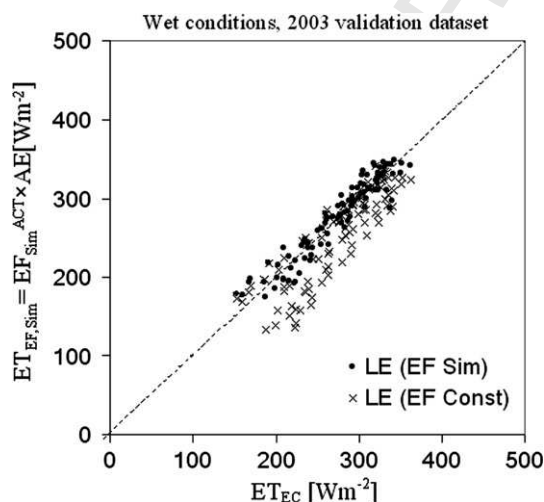$$ET_{EF,Sim} = EF_{Sim}^{ACT}(R_n - G) \qquad (6)$$

Figure 4   Comparison between time course of eddy correlation based EF values and those simulated using the parameterization given in Eqs. (2)–(4) for 10 days period under wet conditions in 2004 season.

Fig. 5 presents a comparison between measured ET values and those simulated using Eq. (6) over the 10-day wet period in 2004. It can be clearly seen that t taking into account the diurnal variation of EF significantly improves ET retrieval. RMSE between measured and simulated ET values was of 18 W m^{-2} and a Nash–Sutcliffe coefficient of 0.9, as compared to 46 W m^{-2} and 0.34, respectively when using a constant EF.

In order to extend this evaluation with independent dataset, a 10-day periods (wet conditions) during 2003 where selected. Fig. 6 shows the comparison between $ET_{EF,Sim}$ and ET_{EC} f including ET estimates when assuming a constant EF. It is shown that the proposed parameterization for EF adequately retrieves the observed values of ET compared to assuming a constant EF during the day. Indeed, RMSE value is about 15 W m^{-2} and the Nash–Sutcliffe coefficient is 0.90. Finally, the interest of the proposed EF parameterization for water balance studies is assessed in terms of

Table 1 Water lost through evapotranspiration during two 10-day wet periods (2004 and 2003, daytime values only); measured, simulated with constant EF and simulated with variable EF

Method	Measured (EC) [mm]	Simulated, Constant EF [mm]	Simulated, Variable EF [mm]
2004	41.3	38.1	41.3
2003	20.9	19.3	21.0

water losses through evapotranspiration during the two wet periods in 2003 and 2004 (Table 1). In both cases, it is shown using a daytime constant EF for the calculation of ET underestimated the amount of water lost through evapotranspiration by 8%. Conversely, using the proposed EF parameterization in the calculation of ET reduces the error on water loss to less than 0.5%.

Parameterizing the AE diurnal course

Implementing Eq. (6) for ET calculation requires the diurnal course of AE = $R_n - G$, which is not routinely available. Various formulations were proposed for estimating AE at a given time of the day (Jackson et al., 1983; Seguin et al., 1989; Bastiaanssen et al., 2000), usually based on sine functions and thus not accounting for any atmospheric disturbance (e.g. Bisht et al., 2005). Another solution is using instantaneous remote sensing observations when ASTER overpasses (11:30 UTC), and then extrapolating the AE diurnal course from parameterizations based on meteorological measurements that remain fairly constant at the scale of the irrigation district.As for the EF parameterization, a heuristic approach is used for the AE diurnal course, by considering surface net radiation without thermal emission component:

$$\left(\frac{(R_n - G)^t}{(R_n - G)^{1130}_{Obs}}\right) = f\left(\frac{R^{*t}}{R^{*1130}}\right) \tag{7}$$

where R^{*t} is a function of solar irradiance ($S^{\downarrow}$) and atmospheric thermal irradiance ($L^{\downarrow}$):

$$R^{*t} = (1 - \alpha)S^{\downarrow t} + \varepsilon L^{\downarrow t} \tag{8}$$

with α and ε surface albedo and emissivity, respectively. They are available from remote sensing and are considered relatively constant throughout the day. $S^{\downarrow}$ is available from meteorological networks or geostationary remote sensors, and $L^{\downarrow}$ can be derived from air temperature and humidity (Brutsaert, 1982). Assuming albedo is constant throughout the day can be far from reality (Jacob and Olioso, 2005), but the validation exercise reported below shows this is not critical for accurately retrieving the AE diurnal course. The 2nd order function f is expressed as:

$$f\left(\frac{R^{*t}}{R^{*1130}}\right) = a_2\left(\frac{R^{*t}}{R^{*1130}}\right)^2 + a_1\left(\frac{R^{*t}}{R^{*1130}}\right) + a_0 \tag{9}$$

Calibrating Eq. (9) over the EC 2004 dataset provided for the coefficients: $a_2 = 0.34285$; $a_1 = 1.15120$; $a_0 = -0.48495$. By incorporating Eqs. (8) and (9) into Eq. (7); half hourly AE

Figure 5 Comparison between measured ET values (ET_{EC}) and those simulated using Eq. (6) for the same 10-days period under wet conditions in 2004 season.

Figure 6 Comparison between ET_{EC} and ET_{Sim} during wet conditions in 2003. ET_{Sim} is calculated both using the proposed parameterization (dots) and, for illustration, using EF_{EC} at 11:30 as constant daytime value (crosses).

441 values are obtained using only diurnal measurements of $S^\downarrow$,
442 $L^\downarrow$, and the single observation $R_n - G_{Obs}^{1130}$ when ASTER over-
443 passes. Fig. 7a and b displays the comparison between ob-
444 served and parameterized AE over the two years (2004 for
445 calibration and 2003 for validation), respectively. For both
446 cases, it is shown the proposed parameterization is ade-
447 quate, with RMSE values ranging from 22 W m^{-2} for the cal-
448 ibration dataset to 30 W m^{-2} for the validation dataset.

Application to ASTER data

450 The proposed parameterizations for the AE and EF diurnal
451 courses rely on standard meteorological data for character-
452 izing the daytime variations, and on remotely sensed obser-
453 vations to account for surface heterogeneities induced by
454 differences in soil moisture and vegetation. Given land sur-
455 face conditions hardly change throughout the day, and
456 cloud free meteorological conditions are almost homoge-
457 neous over the study area, the simulated AE, EF and ET
458 can be considered as representative. It is thus relevant

Figure 7a   Measured vs. simulated available energy during the whole experimental period in 2004.

Figure 7b   Validation of the AE parameterization for the 2003 experimental season.

459 applying this approach to ASTER observations, which 90 m
460 spatial resolution for thermal imagery is amongst the finest
461 possibilities and reduces problems due to mixed pixels
462 (French et al., 2005). Under unstable conditions, an ASTER
463 pixel footprint is larger than the source area for a typical
464 EC system. However, this source area is often located within
465 adjacent ASTER pixels. A footprint analysis is therefore nec-
466 essary before any comparison between remote sensing and
467 in situ observations. To compute the contribution of each
468 part of the source area (i.e. the footprint of the flux mea-
469 surement), several approaches have been developed over
470 the last decades. These range from simple analytical models
471 (e.g. Schuepp et al., 1990) to complex Lagrangian models
472 (e.g. Baldocchi, 1997; Rannik et al., 2000) or models based
473 on large eddy simulations (e.g. Leclerc et al., 1997). As
474 compared to analytical models, the complex models provide
475 more realistic footprint simulations over forest canopies,
476 and they can account for inhomogeneous turbulence. How-
477 ever, they require significantly larger computational power.
478 Despite the lack of complexity, Finn et al. (1996) reported
479 the analytical model proposed by Horst and Weil (1992,
480 1994) produces very similar results to a Lagrangian stochas-
481 tic model, and can therefore be considered as a reliable
482 method. We therefore select this model, which is fully de-
483 scribed over the same study site in Hoedjes et al., 2007.
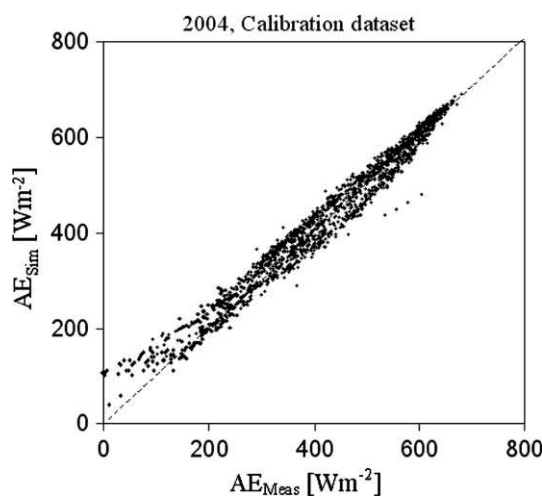
Obtaining fluxes from ASTER observations

485 Calculating land surface net radiation and soil heat flux re-
486 quires apparent albedo (Jacob and Olioso, 2005), broadband
487 emissivity over the [3−100] μm spectral range, and vegeta-
488 tion cover. Albedo (respectively emissivity) is calculated as
489 a linear combination of visible and near infrared reflectance
490 (respectively thermal infrared emissivities), following Jacob
491 et al. (2002) (respectively Ogawa et al. (2003)) for the
492 weighting coefficients. Vegetation cover is computed from
493 Normalized Difference Vegetation Index using the empirical
494 relationship proposed by Asrar et al. (1984), and following
495 Weiss et al., 2002 for implementation. Then, net radiation
496 (R_n^{ASTER}) is classically inferred using ASTER derived albedo,
497 broadband emissivity, and surface radiometric tempera-
498 ture, along with field observations for solar and thermal
499 irradiances. The ratio of soil heat flux (G^{ASTER}) to net radia-
500 tion is calculated according to Santanello and Friedl
501 (2003).Using radiative surface temperature inferred from
502 ASTER imagery, the semi-empirical model proposed by
503 Lhomme et al. (1994) is used to obtain sensible heat flux:

$$H^{ASTER} = \rho c_p \left[\frac{(T_r^{ASTER} - T_a) - c\delta T}{r_a - r_e} \right] \qquad (10)$$

506 where c_p is specific heat of air at constant pressure, ρ is air
507 density, T_a is potential air temperature at reference height
508 (K) and r_a is aerodynamic resistance to heat transfer be-
509 tween the canopy source and the reference height (Brutsa-
510 ert, 1982). Equivalent resistance r_e is given by:

$$r_e = \frac{r_{af} r_{as}}{(r_{af} + r_{as})} \qquad (11)$$

513 where r_{as} is aerodynamic resistance between the soil and
514 the canopy source height (Shuttleworth and Gurney,
515 1990), and r_{af} is canopy bulk boundary layer resistance

(Choudhury and Monteith, 1988). This one source model is based on the bulk aerodynamic relationship, but benefits from a direct use of radiometric surface temperature, instead of aerodynamic surface temperature which is difficult to estimate (Jacob et al., in press). Furthermore, the temperature difference between the soil and the foliage is taken into account through the term $(c\delta T)$, which is given by:

$$\delta T = a(T_r^{ASTER} - T_a)^m \tag{12}$$

and

$$c = \left[\frac{1}{1 + (r_{af}/r_{as})}\right] - f \tag{13}$$

Here f is the fractional vegetation cover, a and m are empirical coefficients ($a = 0.25$ and $m = 2$).

Using the footprint model, EC footprint weighted averages for R_n^{ASTER}, G^{ASTER} and H^{ASTER} are calculated for each ASTER image acquisition. From these average values, the instantaneous EF, AE and Bowen ratio are estimated on ASTER overpass as
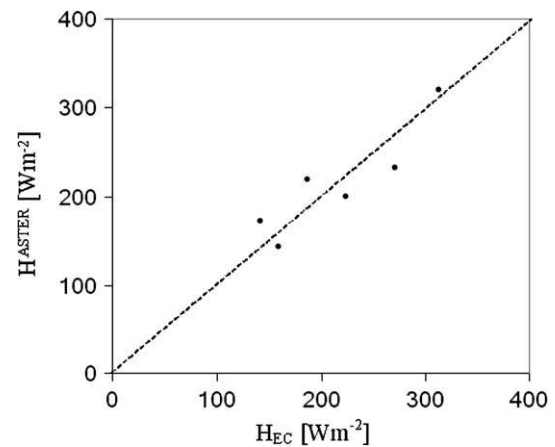
$$AE^{ASTER} = R_n^{ASTER} - G^{ASTER} \tag{14}$$

$$EF^{ASTER} = \frac{R_n^{ASTER} - G^{ASTER} - H^{ASTER}}{R_n^{ASTER} - G^{ASTER}} \tag{15}$$

$$\beta^{ASTER} = \frac{H^{ASTER}}{R_n^{ASTER} - G^{ASTER} - H^{ASTER}} \tag{16}$$
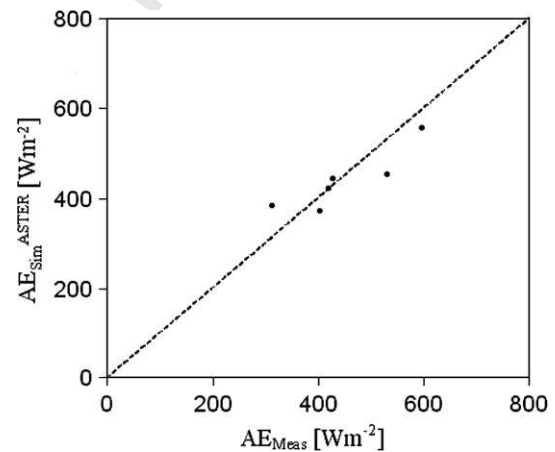
Application of the methods

Fig. 8a and b displays the validation of H^{ASTER} against H_{EC} and of AE^{ASTER} against measured AE, for the 6 ASTER imagery acquisitions. The corresponding RMSE values between ground based and ASTER based estimates were 27 W m^{-2} for H and 51 W m^{-2} for AE. From these estimates, instantaneous EF and Bowen ratio are calculated using Eqs. (15) and (16). A comparison between EF^{ASTER} and EF_{EC} is shown in Fig. 9, the corresponding RMSE value being 0.06. Despite some scatter, results are comparable to those reported in earlier studies (Crow and Kustas, 2005; Batra et al., 2006; Wang et al., 2006). From the calculated Bowen ratio values, it is possible to examine occurrences of wet and dry conditions over the six days of ASTER imagery acquisition. Dry conditions were observed on one day, with $\beta^{ASTER} > 1.5$. On two days, wet conditions were due to irrigation events within one week before ASTER overpasses, with β^{ASTER} from 0.7 to 0.8. On three days, conditions were intermediate, with β^{ASTER} from 1.1 to 1.3.
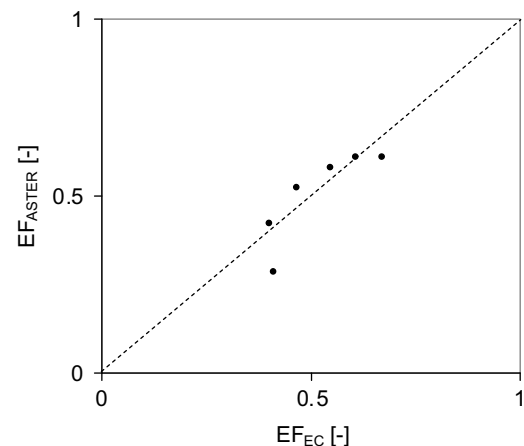
Once inferred, instantaneous EF^{ASTER} is used in place of EF_{Obs}^{1130} in the parameterization scheme (Eqs. (3)–(5)), to obtain r_{EF}^{1130} and consequently the EF diurnal course EF_{Sim}^{ASTER}. Instantaneous AE^{ASTER} is used in Eq. (7) to calculate half-hourly values of AE_{Sim}^{ASTER}. Finally, the ET diurnal course $ET_{EF,Sim}^{ASTER}$ is obtained from Eq. (6) using AE_{Sim}^{ASTER} and EF_{Sim}^{ASTER}. Fig. 10 displays the validation of $ET_{EF,Sim}^{ASTER}$. Linear regression yields $ET_{EF,Sim}^{ASTER} = 0.77 \; ET_{EC} + 53$, with $R^2 = 0.63$ and RMSE = 48 W m^{-2}. These moderate performances can result from 1/amplifications through the ET calculation of errors on remotely sensed variables, 2/assuming daytime albedo is constant which can be far from the reality (Jacob and Olioso, 2005), or 3/the error in H and AE simulations translates

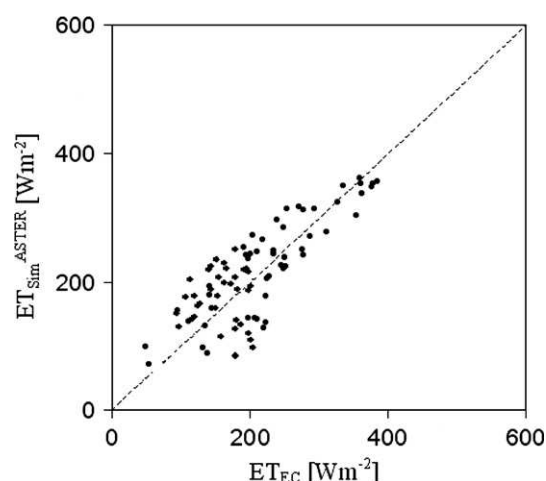**Figure 8a** Comparison between sensible heat fluxes obtained from the eddy covariance system and sensible heat fluxes calculated using the model proposed by Lhomme et al. (1994) combined with ASTER thermal imagery.

Figure 8b Comparison between measured available energy and that simulated using ASTER imagery.

Figure 9 Eddy covariance derived evaporative fraction compared to ASTER derived evaporative fraction.

Figure 10 Latent heat fluxes measured by the EC-system compared to latent heat fluxes calculated using both proposed formulations (for the evaporative fraction and for the available energy) with ASTER data.

569 directly into error in ET since it is estimated as the residual
570 term of the energy balance equation, However, most ap-
571 proaches devoted to estimating ET from remote sensing
572 data are susceptible to comparable errors.

Discussion and conclusion
573

574 Sun synchronous optical remote sensing with high to moder-
575 ate spatial resolution is often used for mapping instanta-
576 neous sensible and latent heat fluxes and evaporative
577 fraction EF. The latter is often assumed to be constant
578 throughout the day, enabling the estimation of daily evapo-
579 transpiration ET provided available energy AE is known. The
580 daytime EF self preservation can be assumed under specific
581 conditions, albeit sensitive to the time when EF is mea-
582 sured. The current study shows although EF remains fairly
583 constant during daytime under dry conditions, but it depicts
584 a concave up shape under wet conditions. Since the latter
585 correspond to large evaporative fluxes, using a constant
586 EF value throughout the day induces large errors in the cal-
587 culation of daily ET.
588   Parameterizing the EF diurnal course from remotely
589 sensed instantaneous estimates is twofold, with the goal
590 of well reproducing a concave up shape under wet condi-
591 tions while EF is self preserved under dry conditions. The
592 first step integrates incoming solar radiation and relative
593 humidity, two main factors for atmospheric demand given
594 air temperature is indirectly considered through relative
595 humidity whereas the impact of wind speed is minor. By first
596 including these two atmospheric factors in the formulation,
597 the EF diurnal course is well reproduced. The second step of
598 the parameterization consists of incorporating land surface
599 condition, since soil moisture and vegetation control the EF
600 absolute value and day-to-day variations. Thus, the day to
601 day variation as well as the spatial heterogeneities is taken
602 into account by correcting EF from remotely sensed instan-
603 taneous ET.
604   This approach seems to include enough information on
605 both atmospheric demand and land surface conditions to ac-

606 count for the diurnal and day-to-day fluctuations of EF — at
607 least — under the prevailing conditions over the study site.
608 However, this parameterization does not include the ET reg-
609 ulation by stomatal conductance. Thus, the relationship
610 developed here is not universal, it needs to be assessed
611 for more diverse ecosytems since plants differently respond
612 to water stress whereas stomatal regulation depends on soil
613 moisture. One might indeed expect that for trees for in-
614 stance the physiological control on stem water storage or
615 release would significantly affect the diurnal course of EF.
616 Either the physiological control in our olive yard is mild in
617 potential conditions, or the empirical equation used to de-
618 rive the diurnal shape of EF takes into account the net ef-
619 fect of EF increase due to lower RH values and stomatal
620 closure in the afternoon. Therefore, despite this empirical
621 feature, the proposed approach is relevant for local applica-
622 tions. Indeed, its implementation over the considered
623 Moroccan olive orchard decreases errors on water consump-
624 tion estimates from 8% to 1% in relative, as compared to
625 assuming EF is self preserved.
626   The next step towards estimating daily ET is deriving the
627 AE diurnal course from a practical relationship. As for EF, a
628 heuristic approach is used, which relies on variables either
629 available from remote sensing data or fairly constant over
630 areas up to several kilometers. Thus, the AE diurnal course
631 is derived from remotely sensed AE when TERRA/ASTER
632 overpasses, to be used along with meteorological observa-
633 tions for incoming shortwave and long wave irradiances.
634 Though the proposed parameterization considers surface al-
635 bedo is constant, the validation emphasizes good perfor-
636 mances, with differences in AE lower than 30 W m^{-2}.
637   Once EF and AE are parameterized, the framework is ap-
638 plied to ASTER data, using a simple energy balance model
639 (Santanello and Friedl, 2003; Lhomme and Elguero, 1999).
640 The methodology is next applied to derive the ET diurnal
641 course. After analyzing the footprint configuration, valida-
642 tion shows performances are comparable to other methods
643 under similar conditions and data availabilities (Crow and
644 Kustas, 2005). As for remote sensing approaches devoted
645 to estimate daily ET, the proposed method is sensitive to er-
646 rors on remotely sensed parameters. However, optimal use
647 of in situ and remote sensing data allows a compromise be-
648 tween loosing (respectively gaining) local (respectively re-
649 gional) information. For operational applications, a
650 temporal sampling of few days is needed. This is currently
651 not possible with high spatial resolution TIR imagery, but
652 could be in the near future. In the meanwhile, disaggrega-
653 tion of low spatial resolution thermal remote sensing data
654 can be a possible solution; however this issue is still subject
655 of ongoing investigations. Finally, it is of interest to mention
656 that this proposed method has been recently applied to a
657 mosaic of agricultural fields in northern Mexico to very
658 encouraging results (Chehbouni et al., 2007c).

References

Abrams, M., 2000. The advanced spaceborne thermal emission and reflection radiometer (ASTER): data products for the high spatial resolution imager on NASA's Terra platform. International Journal of Remote Sensing 21 (5), 847–859.

Abrams, M., Hook, S., 2002. ASTER User Handbook Jet Propulsion Laboratory. Pasadena, California, 135 pp.

Allen, R.G., 2000. Using the FAO-56 dual crop coefficient method over an irrigated region as part of an evapotranspiration intercomparison study. Journal of Hydrology 229, 27–41.

Allen, R.G., Tasumi, M., Trezza, R., 2007. Satellite-based energy balance for mapping evapotranspiration with internalized calibration (METRIC) – model. Journal of Irrigation and Drainage Engineering 133 (4), 380–394.

Asrar, G., Fuchs, M., Kanemasu, E.T., Hatfield, J.L., 1984. Estimating absorbed photosynthetic radiation and leaf area index from spectral reflectance in wheat. Agronomy Journal 76, 300–306.

Baldocchi, D., 1997. Flux footprints within and over forest canopies. Boundary-Layer Meteorology 85, 273–292.

Baldocchi, D.D., Xu, L.K., Kiang, N., 2004. How plant functional-type, weather, seasonal drought, and soil physical properties alter water and energy fluxes of an oak-grass savanna and an annual grassland. Agricultural and Forest Meteorology 123, 13–39.

Bastiaanssen, W.G.M., Menenti, M., Feddes, R.A., Holtslag, A.A., 1998. A remote sensing surface energy balance algorithm for land (SEBAL): I. Formulation.. Journal of Hydrology 212–213 (1–4), 198–212.

Bastiaanssen, W.G.M., Molden, D.J., Makin, I.W., 2000. Remote sensing for irrigated agriculture: examples from research and possible applications. Agricultural Water Management 46, 137–155.

Batra, N., Islam, S., Venturini, V., Bisht, G., Jiang, L., 2006. Estimation and comparison of evapotranspiration from MODIS and AVHRR sensors for clear sky days over the Southern Great Plains. Remote Sensing of Environment 103, 1–15.

Bisht, G., Venturini, V., Jiang, L., Islam, S., 2005. Estimation of the net radiation using MODIS (moderate resolution imaging spectroradiometer) data for clear sky days. Remote Sensing of Environment 97, 52–67.

Braud, I., Dantas Antonino, A.C., Vauclin, M., Thony, J.L., Ruelle, P.A., 1995. Simple Soil Plant Atmosphere Transfer model (SiSPAT) development and field verification. Journal of Hydrology 166, 213–250.

Brutsaert, W., 1982. Evaporation into the Atmosphere. Reidel, Dordrecht, 299 pp.

Calvet, J.-C., Noilhan, J., Roujean, J.-L., Bessemoulin, P., Cabelguenne, M., Olioso, A., Wigneron, J.-P., 1998. An interactive vegetation SVAT model tested against data from six contrasting sites. Agricultural and Forest Meteorology 92, 73–95.

Caparrini, F., Castelli, F., Entekhabi, D., 2003. Mapping of land-atmosphere heat fluxes and surface parameters with remote sensing data. Boundary-Layer Meteorology 107, 605–633.

Caparrini, F., Castelli, F., Entekhabi, D., 2004. Variational estimation of soil and vegetation turbulent transfer and heat flux parameters from sequences of multisensor imagery. Water Resources Research 40, W12515. doi:10.1029/2004WR00335.

Chandrapala, L., Wimalasuriya, M., 2003. Satellite measurements supplemented with meteorological data to operationally estimate evaporation in Sri Lanka. Agricultural Water Management 58, 89–107.

Chaponnière, A., Boulet, G., Chehbouni, A., Aresmouk, M., 2007. Understanding hydrological processes with scarce data in a mountain environment. Hydrological Processes. doi:10.1002/hyp.677.

Chehbouni, A., Escadafal, R., Boulet, G., Duchemin, B., Simonneaux, V., Dedieu, G., Mougenot, B., Khabba, S., Kharrou, H.,

Merlin, O., Chaponnière, A., Ezzahar, J., Er-Raki, S., Hoedjes, J., Hadria, R., Abourida, H., Cheggour, A., Raibi, F., Hanich, L., Guemouria, N., Chehbouni, Ah., Olioso, A., Jacob, F. and Sobrino, J., in press-a. The Use of Remotely Sensed data for Integrated Hydrological Modeling in Arid and Semi-Arid Regions: the SUDMED Program. International Journal of Remote Sensing. Q2

Chehbouni, A., Ezzahar, J., Watts, C., Rodriguez, J.-C., Garatuza-Payan, J., in press-b. Estimating area-averaged surface fluxes over contrasted agricultural patchwork in a semi-arid region. In: Joachim Hill, Achim Röder (Eds.), Advances in Remote Sensing and Geoinformation Processing for Land Degradation Assessment, Taylor and Francis.

Chehbouni, A., Hoedjes, J., Rodriquez, J.-C., Watts, C., Garatuza, J., Jacob, F., Kerr, Y.H., 2007c. Using remotely sensed data to estimate area-averaged daily surface fluxes over a semi-arid mixed agricultural land. Agricultural and Forest Meteorology. doi:10.1111/j.1365-2486.2007.01466.

Choudhury, B.J., Monteith, J.L., 1988. A four-layer model for the heat budget of homogeneous land surfaces. Quarterly Journal of the Royal Meteorological Society 114, 373–398.

Cleugh, H.A., Leuning, R., Mu, Q., Running, S.W., 2007. Regional evaporation estimates from flux tower and MODIS satellite data. Remote Sensing of Environment 106, 285–304.

Coudert, B., Ottlé, C., Boudevillain, B., Demarty, J., Guillevic, P., 2006. Contribution of Thermal Infrared remote sensing data in multiobjective calibration of a dual source SVAT model. Journal of Hydrometeorology 7 (3), 404–420.

Crago, R.D., 1996. Conservation and variability of the evaporative fraction during daytime. Journal of Hydrology 180, 173–194.

Crago, R.D., Brutsaert, W., 1996. Daytime evaporation and the self-preservation of the evaporative fraction and the Bowen ratio. Journal of Hydrology 178, 241–255.

Crow, W.T., Kustas, W.P., 2005. Utility of assimilating surface radiometric temperature observations for evaporative fraction and heat transfer coefficient retrieval. Boundary-Layer Meteorology 115, 105–130.

Duchemin, B., Hadria, R., Er-Raki, S., Boulet, G., Maisongrande, P., Chehbouni, A., Escadafal, R., Ezzahar, J., Hoedjes, J., Kharrou, M.H., Khabba, S., Mougenot, B., Olioso, A., Rodriguez, J-C., Simonneaux, V., 2006. Monitoring wheat phenology and irrigation in Center of Morocco: on the use of relationship between evapotranspiration, crops coefficients, leaf area index and remotely-sensed vegetation indices. Agricultural Water Management 79, 1–27.

Er-Raki, S., Chehbouni, A., Guemouria, N., Duchemin, B., Ezzahar, J., Hadria, R., 2007a. Combining FAO-56 model and ground-based remote sensing to estimate water consumptions of wheat crops in a semi-arid region. Agricultural water management 87, 41–54.

Er-Raki, S., Chehbouni, A., Hoedjes, J., Ezzahar, J., Duchemin, B., Jacob, F., 2007b. Assimilation of ASTER based ET estimates in FAO 56 model over olive orchards in a semi-arid region. Agricultural water management. doi:10.1016/j.agwat.2007.10.01.

Finn, D., Lamb, B., Leclerc, M.Y., Horst, T.W., 1996. Experimental evaluation of analytical and Lagrangian surface-layer footprint models. Boundary-Layer Meteorology 80, 283–308.

French, A.N., Jacob, F., Anderson, M.C., Kustas, W.P., Timmermans, W., Gieske, A., Su, B., Su, H., McCabe, M.F., Li, F., Prueger, J., Brunsell, N., 2005. Surface energy fluxes with the Advanced Spaceborne Thermal Emission and Reflection radiometer (ASTER) at the Iowa 2002 SMACEX site (USA). Remote Sensing of Environment 99, 55–65.

Fujisada, H., 1998. ASTER Level-1 data processing algorithm. IEEE Transactions on Geoscience and Remote Sensing 36, 1101–1112.

Fujisada, H., Sakuma, F., Ono, A., Kudoh, M., 1998. Design and preflight performance of ASTER instrument protoflight model.

IEEE Transactions on Geoscience and Remote Sensing 36 (4), 1152–1160.

Gentine, P., Entekhabi, D., Chehbouni, A., Boulet, G., Duchemin, B., 2007. Analysis of evaporative fraction diurnal behaviour. Agricultural and Forest Meteorology 143, 13–29.

Gillespie, A., Rokugawa, S., Matsunaga, T., Cothern, J.S., Hook, S.J., Kahle, A.B., 1998. A temperature and emissivity separation algorithm for Advanced Spaceborne Thermal Emission and Reflection Radiometer (ASTER) images. IEEE Transactions on Geoscience and Remote Sensing 36 (4), 1113–1126.

Glenn, E.P., Huete, A.R., Nagler, P.L., Hirschboeck, K.K., Brown, P., 2007. Integrating remote sensing and ground methods to estimate evapotranspiration. Critical Reviews in Plant Sciences 26 (3), 139–168.

Gomez, M., Sobrino, J., Olioso, A., Jacob, F., 2005. Retrieval of evapotranspiration over the Alpilles test site using PolDER and thermal camera data. Remote Sensing of Environment 96, 399–408.

Hoedjes, J.C.B., Zuurbier, R.M., Watts, C.J., 2002. Large aperture scintillometer used over a homogeneous irrigated area, partly affected by regional advection. Boundary-Layer Meteorology 105, 99–117.

Hoedjes, J.C.B., Chehbouni, A., Ezzahar, J., Escadafal, R., De Bruin, H.A.R., 2007. Comparison of large aperture scintillometer and Eddy covariance measurements: can thermal infrared data be used to capture footprint induced differences? Journal of Hydrometeorology 8, 144–159.

Horst, T.W., Weil, J.C., 1992. Footprint estimation for scalar flux measurements in the atmospheric surface layer. Boundary-Layer Meteorology 59, 279–296.

Horst, T.W., Weil, J.C., 1994. How far is far enough?: The fetch requirements for micrometeorological measurement of surface fluxes. Journal of Oceanic and Atmospheric Technology 11, 1018–1025.

Jackson, R.D., Reginato, R.J., Idso, S.B., 1977. Wheat canopy temperature: a practical tool for evaluating water requirements. Water Resources Research 13, 651–656.

Jackson, R.D., Hatfield, J.L., Reginato, R.J., Idso, S.B., Pinter Jr., P.J., 1983. Estimation of daily evapotranspiration from one time-of-day measurements. Agricultural Water Management 7, 351–362.

Jacob, F., Weiss, M., Olioso, A., French, A., 2002. Assessing the narrowband to broadband conversion to estimate visible, near infrared and shortwave apparent albedo from airborne PolDER data. Agronomie: Agriculture and Environment 22, 537–546.

Jacob, F., Petitcolin, F., Schmugge, T., Vermote, E., French, A., Ogawa, K., 2004. Comparison of land surface emissivity and radiometric temperature derived from MODIS and ASTER sensors. Remote Sensing of Environment 90, 137–152.

Jacob, F., Olioso, A., 2005. Derivation of diurnal courses of albedo and reflected solar irradiance from airborne POLDER data acquired near solar noon. Journal of Geophysical Research 110, D10104. doi:10.1029/2004JD00488.

Jacob, F., Schmugge, T., Olioso, A., French, A., Courault, D., Ogawa, K., Petitcolin, F., Chehbouni, G., Pinheiro, A., Privette, J., in press. Modeling and inversion in thermal infrared remote sensing over vegetated land surfaces. In: Advances in Land Remote Sensing: System, Modeling, Inversion and Application (S. Liang Ed.), Springer.

Q5 Leclerc, M.Y., Shen, S., Lamb, B., 1997. Observations and large-Eddy simulation modeling of footprints in the lower convective boundary layer. Journal of Geophysical Research 120, 9323–9334.

Lhomme, J.-P., Monteny, B., Amadou, M., 1994. Estimating sensible heat flux from radiometric temperature over sparse millet. Agricultural and Forest Meteorology 68, 77–91.

Lhomme, J.-P., Elguero, E., 1999. Examination of evaporative fraction diurnal behaviour using a soil-vegetation model coupled with a mixed-layer model. Hydrology and Earth System Sciences 3 (2), 259–270.

Li, S.-G., Eugster, W., Asanuma, J., Kotani, A., Davaa, G., Oyunbaatar, D., Sugita, M., 2006. Energy partitioning and its biophysical controls above a grazing steppe in central Mongolia. Agricultural and Forest Meteorology 137 (1–2), 89–106.

Liu, Y., Hiyama, T., Yamaguchi, Y., 2006. Scaling of land surface temperature using satellite data: a case examination on ASTER and MODIS products over a heterogeneous terrain area. Remote Sensing of Environment 105, 115–128.

Mahfouf, J.F., Manzi, A.O., Noilhan, J., Giordani, H., Déqué, M., 1995. The land surface scheme ISBA within the Météo-France climate model ARPEGE. Part I. Implementation and preliminary results.. Journal of Climate 8, 2039–2057.

Mu, Q., Heinsch, F.A., Zhao, M., Running, S.W., 2007. Development of a global evapotranspiration algorithm based on MODIS and global meteorology data. Remote Sensing of Environment 111 (4), 519–536.

Nichols, W.E., Cuenca, R.H., 1993. Evaluation of the evaporative fraction for parameterization of the surface, energy-balance. Water Resources Research 29, 3681–3690.

Norman, J.M., Anderson, M.C., Kustas, W.P., French, A.N., Mecikalski, J., Torn, R., Diak, G.R., Schmugge, T.J., Tanner, B.C.W., 2003. Remote sensing of surface energy fluxes at 10^1-m pixel resolutions. Water Resources Research 39 (8), 1221. doi:10.1029/2002WR00177.

Ogawa, K., Schmugge, T., Jacob, F., French, A., 2003. Estimation of land surface window (8–12 μm) emissivity from multi-spectral thermal infrared remote sensing-A case study in a part of Sahara Desert. Geophysical Research Letters 30, 1067–1071.

Ohmura, A., Wild, M., 2002. Is the hydrological cycle accelerating? Science 298, 1345–1346.

Olioso, A., Carlson, T.N., Brisson, N., 1996. Simulation of diurnal transpiration and photo-synthesis of a water stressed soybean crop. Agricultural and Forest Meteorology 81, 41–59.

Olioso, A., Inoue, Y., Ortega-Farias, S., Demarty, J., Wigneron, J.-P., Braud, I., Jacob, F., Lecharpentier, P., Ottlé, C., Calvet, J.-C., Brisson, N., 2005. Future directions for advanced evapotranspiration modeling: assimilation of remote sensing data into crop simulation models and SVAT models. Irrigation and Drainage Systems 19 (3–4), 355–376.

Porporato, A., Daly, E., Rodriguez-Iturbe, I., 2004. Soil water balance and ecosystem response to climate change. American Naturalist 164, 625–632.

Rannik, Ü., Aubinet, M., Kurbanmuradov, O., Sabelfeld, K.K., Markkanen, T., Vesala, T., 2000. Footprint analysis for measurements over a heterogeneous forest. Boundary-Layer Meteorology 97, 137–166.

Roerink, G.J., Su, Z., Menenti, M., 2000. S-SEBI: a simple remote sensing algorithm to estimate the surface energy balance. Physics and Chemistry of the Earth (B) 25 (2), 147–157.

Santanello, J.A., Friedl, M.A., 2003. Diurnal covariation in soil heat flux and net radiation. Journal of Applied Meteorology 42, 851–862.

Schmugge, T., Hook, S.J., Coll, C., 1998. Recovering surface temperature and emissivity from thermal infrared multispectral data. Remote Sensing of Environment 65 (2), 121–131.

Schuepp, P.H., Leclerc, M.Y., MacPherson, J.I., Desjardins, R.L., 1990. Footprint prediction of scalar fluxes from analytical solutions of the diffusion equation. Boundary-Layer Meteorology 50, 355–373.

Schuurmans, J.M., Troch, P.A., Veldhuizen, A.A., Bastiaanssen, W.G.M., Bierkens, M.F.P., 2003. Assimilation of remotely sensed latent heat flux in a distributed hydrological model. Advances in Water Resources 26, 151–159.

Seguin, B., Assad, E., Freteaud, P., Imbernon, J.-P., Kerr, Y.H., Lagouarde, J.-P., 1989. Use of meteorological satellites for

935   water balance monitoring in Sahelian regions. International
936   Journal of Remote Sensing 10, 1001—1017.
937   Shuttleworth, W.J., Gurney, R.J., Hsu, A.Y., Ormsby, J.P.,
938   1989FIFE: The Variation in Energy Partition at Surface Flux
939   Sites, vol. 186. IAHS Publication, pp. 67—74.
940   Shuttleworth, W.J., Gurney, R.J., 1990. The theoretical relation-
941   ship between foliage temperature and canopy resistance in
942   sparse crops. Quarterly Journal of the Royal Meteorological
943   Society 116, 497—519.
944   Sugita, M., Brutsaert, W., 1991. Daily evaporation over a region
945   from lower boundary layer profiles. Water Resources Research
946   27, 747—752.
947   Suleiman, A., Crago, R.D., 2004. Hourly and daytime evapotrans-
948   piration from grassland using radiometric surface temperatures.
949   Agronomy Journal 96, 384—390.
950   Twine, T.E., Kustas, W.P., Norman, J.M., Cook, D.R., Houser, P.R.,
951   Meyers, T.P., Prueger, J.H., Starks, P.J., Wesely, M.L., 2000.
952   Correcting Eddy-covariance flux underestimates over a grass-
953   land. Agricultural and Forest Meteorology 103, 279—300.
954   Thome, K., Palluconi, F., Takashima, T., Masuda, K., 1998.
955   Atmospheric correction of ASTER. IEEE Transactions on Geosci-
956   ence and Remote Sensing 36, 1199—1211.
957   Van den Hurk, B.J.J.M., Bastiaanssen, W.G.M., Pelgrum, H., Van
958   Meijgaard, E., 1997. A new methodology for initialization of soil
959   moisture fields in numerical weather prediction models using
960   METEOSAT and NOAA data. Journal of Applied Meteorology 36,
961   1271—1283.
962   Van Dijk, A., Moene, A.F. De Bruin, H.A.R., 2004. The principles of
963   surface flux physics: theory, practice and description of the
964   ECPACK library. Internal Report 2004/1, Meteorology and Air

965   Quality Group, Wageningen University, Wageningen, The Neth-
966   erlands, 99 pp.
967   Wang, K., Li, Z., Cribb, M., 2006. Estimation of evaporative
968   fraction from a combination of day and night land surface
969   temperatures and NDVI: a new method to determine the
970   Priestley-Taylor parameter. Remote Sensing of Environment
971   102, 293—305.
972   Weiss, M., Jacob, F., Baret, F., Pragnère, A., Bruchou, C., Leroy,
973   M., Hautecoeur, O., Prévot, L., Bruguier, N., 2002. Evalutation
974   of kernel-driven BRDF models for the normalization of Alpilles/
975   ReSeDA POLDER data. Agronomie 22, 531—536.
976   Wild, M., Ohmura, A., Gilgen, H., Rosenfeld, D., 2004. On the
977   consistency of trends in radiation and temperature records and
978   implications for the global hydrological cycle. Geophysical
979   Research Letters 31, L11201. doi:10.1029/2003GL01918.
980   Williams, D.G., Cable, W., Hultine, K., Hoedjes, J.C.B., Yepez,
981   E.A., Simonneaux, V., Er-Raki, S., Boulet, G., De Bruin, H.A.R.,
982   Chehbouni, A., Hartogensis, O.K., Timouk, F., 2004. Evapo-
983   transpiration components determined by stable isotope, sap
984   flow and eddy covariance techniques. Agricultural and Forest
985   Meteorology 125, 241—258.
986   Yang, F., White, M.A., Michaelis, A.R., Ichii, K., Hashimoto, H.,
987   Votava, P., Zhu, A-X., Nemani, R.R., 2006. Prediction of
988   continental-scale evapotranspiration by combining MODIS and
989   AmeriFlux data through support vector machine. IEEE Trans-
990   actions on Geoscience and Remote Sensing 44 (11), 3452—
991   3461.
992   Zhang, L., Lemeur, R., 1995. Evaluation of daily evapotranspiration
993   estimates from instantaneous measurements. Agricultural and
994   Forest Meteorology 74, 139—154.
995